atmosphere

MDPI

Article

Long-Term Changes of Source Apportioned Particle Number Concentrations in a Metropolitan Area of the Northeastern United States

Stefania Squizzato [1,2], Mauro Masiol [1,2], Fereshteh Emami [2,3], David C. Chalupa [4], Mark J. Utell [4,5], David Q. Rich [1,4,5] and Philip K. Hopke [1,2,*]

1 Department of Public Health Sciences, University of Rochester Medical Center, Rochester, NY 14642, USA; stefania.squizzato81@gmail.com (S.S.); mauro.masiol@gmail.com (M.M.); david_rich@URMC.rochester.edu (D.Q.R.)
2 Center for Air Resources Engineering and Science, Clarkson University, Potsdam, NY 13699, USA; fereshteh.emami@selu.edu
3 Department of Chemistry and Physics, Southeastern Louisiana University, Hammond, LA 70402, USA
4 Department of Environmental Medicine, University of Rochester Medical Center, Rochester, NY 14642, USA; david_chalupa@URMC.rochester.edu (D.C.C.); mark_utell@URMC.rochester.edu (M.J.U.)
5 Department of Medicine, University of Rochester Medical Center, Rochester, NY 14642, USA
* Correspondence: phopke@clarkson.edu

Received: 20 November 2018; Accepted: 9 January 2019; Published: 12 January 2019

Abstract: The northeastern United States has experienced significant emissions reductions in the last two decades leading to a decrease in $PM_{2.5}$, major gaseous pollutants (SO_2, CO, NO_x) and ultrafine particles (UFPs) concentrations. Emissions controls were implemented for coal-fired power plants, and new heavy-duty diesel trucks were equipped with particle traps and NO_x control systems, and ultralow sulfur content is mandatory for both road and non-road diesel as well as residual oil for space heating. At the same time, economic changes also influenced the trends in air pollutants. Investigating the influence of these changes on ultrafine particle sources is fundamental to determine the success of the mitigation strategies and to plan future actions. Particle size distributions have been measured in Rochester, NY since January 2002. The particle sources were investigated with positive matrix factorization (PMF) of the size distributions (11–470 nm) and measured criteria pollutants during five periods (2002–2003, 2004–2007, 2008–2010, 2011–2013, and 2014–2016) and three seasons (winter, summer, and transition). Monthly, weekly, and hourly source contributions patterns were evaluated.

Keywords: ultrafine particles; source apportionment; long-term trends; air pollution

1. Introduction

In the United States, criteria air pollutants, including particulate matter, are measured at fixed air quality monitoring stations in the National Ambient Air Quality Standards (NAAQS) compliance monitoring network managed by state, local, or tribal agencies [1]. Despite the number of stations measuring air quality, limited data are still available for some air pollutants, including submicron particles (SMPs, <1 μm) and ultrafine particles (UFPs, <100 nm), which are associated with adverse effects upon human health (e.g., [2–7]). Submicron particles may include primary particles emitted from many anthropogenic activities, natural sources, and/or secondary particles formed by gas-to-particle conversion processes, including nucleation and condensation (e.g., [8–11]). Although UFPs account for most of the particle number concentrations (PNCs), they generally have negligible mass and therefore, do not correlate well with the PM mass [12]. In urban environments, UFPs are primarily

emitted by fossil fuel combustion from sources such as motor vehicles (e.g., [13,14]), maritime, rail, and airport emissions (e.g., [15–17]), industrial emissions [18], space heating [19], waste incineration [20], and biomass burning [21]. There can also be non-combustion sources (e.g., [22]) and new particle formation [8,12].

The northeastern United States has experienced significant emissions reductions over the past two decades leading to decreases in $PM_{2.5,}$ major gaseous pollutants (SO_2, CO, NO_x) [23–25] and UFPs concentrations [26–28]. Emission controls were implemented on coal-fired power plants, and new heavy-duty diesel trucks were equipped with particle traps and NO_x control systems. Ultralow sulfur content was mandated for both road and non-road diesel fuel as well as for residual oil used for space heating in New York State after 1 July 2012. During the same period as these policy implementations were taking effect, economic changes also influenced the trends in air pollutants [24,25,28]. These changes were largely due to a shift from coal to natural gas for electricity production. Thus, investigating the influence of these changes in the sources of ultrafine particles, and determining their impacts on ultrafine particle sources is fundamental to assess the success of the mitigation strategies and to plan future actions.

Particle number size distributions (PNSDs) have been measured in Rochester, NY since January 2002. Ogulei et al. [29] performed the initial assessment of the particle sources in Rochester by applying a Positive Matrix Factorization model using PMF2 to the measured PNSDs and pollutant gases measured from late 2004 to near the end of 2005. Kasumba et al. [30] extended the study including the analysis of data collected from January 2002 and extending the analysis to the end of 2007. More than 80% of the apportioned PNCs were attributed to traffic, nucleation, and industrial emissions sources. Other identified sources were residential/commercial heating, secondary nitrate, secondary sulfate, O_3-rich secondary aerosol, and regionally transported aerosol.

This study apportioned the sources of PNSDs by analyzing the data collected between 2008 and 2016. Diel and day of the week source contribution patterns were evaluated to support source profiles interpretation. Changes in source profiles were interpreted considering the mitigation strategies implemented from 2002 to 2016 as well as the effects of the economic drivers (e.g., the 2008 financial crisis and lower price for natural gas).

2. Material and Methods

2.1. Study Area and Sampling Location

Rochester is located on the southern shore of Lake Ontario. In addition to typical urban sources (road traffic, domestic heating from natural gas), several other sources operate: (i) Residential wood combustion was estimated to account for 17–30% of the winter $PM_{2.5}$ mass [31]; (ii) industrial emissions from a coal-fired cogeneration plant (Kodak Park complex, now Eastman Business Park) whose production decreased substantially during recent years and will be converted to natural gas in 2018; (iii) off-road transport (i.e., diesel rail, shipping traffic on Lake Ontario, and emissions from the international airport), and (iv) wastewater treatment plants. A 260 MW coal-fired power plant was shut down in April 2008. The coal-fired power plant and the Kodak Park cogeneration plant were the dominant industrial UFP emission sources prior to 2008 [24,27,28].

2.2. Experimental Section

PNSDs were measured from January 2002 to February 2004 at a site in downtown Rochester (FIR: USEPA site code 36-055-6001; 43°09′40″ N, 77°36′12″ W). This site was closed in March 2004, and in May 2004, was moved to the current location of the New York State Department of Environmental Conservation (NYS DEC) site (DEC: USEPA site code 36–055-1007; 43°08′46″ N, 77°32′52″ W). The DEC site is in a residential environment close to two major highways (I-490 and I-590) and a major state route (NY 96) (Figure 1). The main railroad line through Rochester is adjacent to the site. PNSDs were measured using a scanning mobility particle sizer (SMPS) consisting of a TSI model 3071 differential

mobility analyzer and a TSI model 3010 condensation particle counter over the size range of 10.4 nm (lower) to 542 nm (upper) with a scan time of 5 min per sample. The monitoring system was described in detail by Kasumba et al. [30] and Masiol et al. [28]. The 5 minute measurements were averaged to hourly values for further analysis. Hourly CO, $PM_{2.5}$, SO_2, O_3, NO, NO_2, NO_y, black carbon measured at 880 nm (BC) and at 370 nm (UVBC) and Delta-C (DC = UVBC–BC) concentrations were measured by the NYS Department of Environmental Conservation (DEC). Details of gases, $PM_{2.5}$, BC, and UVBC measurements were provided by Emami et al. [24]. BC and UVBC measurements started in 2008 and NO, NO_2, and NOy have only been monitored since late 2010. Although CO has been measured since 2002, there was a high percentage of below detection limit CO data during 2008–2010. Therefore, CO was not included in the PMF analysis. A new, more sensitive CO monitor was installed in late 2010 providing useful concentrations for the subsequent periods. A new SO_2 monitor was also installed at the same time as the new CO, NO_x, and NO_y monitors. Ozone data were available throughout the particle number measurement period.

Figure 1. Location of the sampling sites and major coal-fired facilities in Rochester, New York (NY).

2.3. Data Analysis

PMF analysis was performed by using the US EPA PMF V5 on the 1 hour averaged sized number concentrations and total number concentrations derived from the SMPS data combined with the hourly concentrations of the gaseous pollutants (CO, SO_2, NO, NO_2, NO_y), $PM_{2.5}$, BC, and Delta-C, depending on their availability. The presence of additional species in the datasets can help to separate and identify additional sources and can decrease the rotational ambiguity because of the increased numbers of edge points [32]. The previously reported analyses were not repeated. Thus, these additional analyses began at the start of 2008. The 2008–2016 period was divided into three sub-periods (2008–2010, 2011–2013, and 2014–2016). The three sub-periods were defined in part by the availability of auxiliary data. For 2008–2010, there were no CO values above the detection limit of the monitor, but values were available once the new, more sensitive unit was installed in late 2010 with the NO_x, NO_y, and more sensitive SO_2 monitors. Given the potential changes in the sources occurring between 2008 and 2013, the 2014–2016 period was treated separately as was done by Squizzato et al. [25] for all of the pollutants across New York State.

Prior work by Zhou et al. [33,34] and by Ogulei et al. [29] had shown that there are sufficient changes in the source profiles over the course of the year due to changing temperatures and photochemical activity. Thus, the PMF analyses were performed seasonally (winter: Dec-Jan-Feb;

summer: Jun-Jul-Aug; transition: Mar-Apr-May-Sep-Oct-Nov) similar to Kasumba et al. [30] who found solutions that were similar to the prior separated seasonal results [29].

PMF details have been provided elsewhere [35–37]. All missing concentrations were replaced by the median value for the given size bin or species and their uncertainties were set at four times the value. The particle number concentration uncertainties were estimated from the following equation [38]:

$$\sigma_{ij} = \alpha(N_{ij} + \overline{N}_j) \quad (1)$$

where σ is the calculated (estimated) measurement error; α = 0.01; N is the observed number concentration; and $\overline{N}$ is the arithmetic mean of the reported values N. The ultimate uncertainties inputted into US EPA PMF were computed based on the measurement errors with the expression:

$$s_{ij} = \sigma_{ij} + C_3(N_{ij}) \quad (2)$$

where C_3 is a constant chosen based on the prior studies to be 0.1 except for the summer data from 2011 to 2013, where it was set at 0.2 because there was more variability observed in these data. For the gaseous species and $PM_{2.5}$, the specifications for each monitor provided a method detection limit (MDL) and the calibration uncertainties were set at 7%. The approach of Polissar et al. [39] was then applied to calculate the uncertainties. Because of the uncertainties in the mass absorption coefficients used in the aethalometer measurements at 370 and 880 nm, the measurement error was set at 15% and combined with the reported MDLs to provide the uncertainties. The errors in DC were calculated by propagating the errors in the two BC values. Species measured below detection limits (DL) were replaced by 1/2 DL and assigned an uncertainty equal to 5/6 DL [39]. The total particle number concentration for each hour were set as the "Total Variable" and the f-values for total PNC were used to normalize the size bin data and the contributions. The other variables were left as their values normalized to mean G value equal to 1.

The best solutions were identified according to the generally accepted criteria and guidelines [37,40–42] including: (i) Knowledge of sources affecting the study area, (ii) the Q-value with respect to the expected (theoretical) value and its stability over multiple runs (n = 200), (iii) the number of absolute scaled residuals greater than ±3, and (iv) finding profile uncertainties calculated by bootstrap (BS, n = 200) and displacement (DISP) methods within an acceptable range [43].

3. Results and Discussion

3.1. Identified Sources and Temporal Variability

Different sources were extracted during each season because of the temporal variability of both primary particle sources and gas-to-particle formation processes. The most plausible solutions for each period and each season were chosen considering: (i) Appropriately narrow distributions of the scaled residuals; (ii) all runs converged; (iii) stable Q values over 200 runs; and (iv) Qtrue/Qexp ratio ~1; (v) fewer swaps in bootstrap analysis over 200 runs and no unmapped factors; (vi) no swaps in displacement analysis (DISP); and (vii) the most physically interpretable results.

For the 2002–2007 period, Kasumba et al. [30] identified 7 factors for winter; 8 factors for summer and the 2002–2003 transition; and 9 factors for the 2004–2007 transition (Table 1). Overall, nucleation, two traffic factors (traffic 1 and traffic 2), O_3-rich secondary aerosol, and the industrial sources were extracted for all seasons. Additional identified sources were secondary nitrate and residential/domestic heating (winter and transition), secondary sulfate and a mixed source (transition and summer), and regionally transported aerosol (summer only).

Generally, similar results were obtained for the three seasons in the 2008–2016 period. However, the number of factors were found to decrease and the industrial and the mixed sources were no longer identified. These differences reflect the changes in sources during the 2005 to 2007 period. Significant reductions in SO_2 and particle emissions included the early 2008 closure of the coal-fired

power plant, the reduction of the coal-fired cogeneration plant activity, and reductions in sulfur content for on-road diesel fuel in late 2006. These changes likely resulted in the elimination of the industrial and mixed sources. In summary, for the 2002–2016 period, four sources were identified for all seasons: Nucleation, two traffic factors (traffic 1 and traffic 2), and O_3-rich secondary aerosol. Secondary nitrate and residential/commercial heating were identified only during winter and transition. Secondary sulfate was resolved only during summer and transition. Regionally transported aerosol was a summer only source. As an illustrative example, the profiles for the winter 2011–2013 period are presented in Figure 2. All of the profiles of the identified sources over the whole 2002 to 2016 period are provided by season in the Supplementary Materials (Figures S1 to S19). Table 1 reports the average PNC source contributions during the five periods. Figure 3 presents the seasonal distributions of the commonly identified PSD source contributions while Figure S20 presents the distributions for the mixed, regional, and industrial sources. Figures 4–6 present the diel variations in the source contributions. Figures S21 to S23 present the day of the week variations for each source by season and by period. The sources are discussed individually in the next section.

Table 1. Source contributions in percentage to particle number concentrations (PNC) by season and by period.

Season	Period	Nucleation (%)	Traffic 1 (%)	Traffic 2 (%)	O_3-Rich (%)	Residential/Commercial Heating (%)	Secondary Nitrate (%)	Secondary Sulfate (%)	Regional Transported (%)	Industrial (%)	Mixed (%)
Winter	2002–2003	20	29	16	2	6	1			25	
	2004–2007	19	26	17	2	8	2			26	
	2008–2010	19	32	24	4	16	5				
	2011–2013	23	39	26	6	3	4				
	2014–2016	25	34	17	6	16	1				
Transition	2002–2003	20	23	10	3	4	1			17	23
	2004–2007	11	18	14	2	10	3	2		18	21
	2008–2010	15	28	20	3	0	3	30			
	2011–2013	15	27	19	3	3	6	27			
	2014–2016	18	28	4	9	19	2	21			
Summer	2002–2003	19	20	14	2			7	2	18	19
	2004–2007	13	19	15	4			8	2	18	20
	2008–2010	29	24	29	3			5	9		
	2011–2013	24	34	29	6			2	5		
	2014–2016	22	26	28	14			7	4		

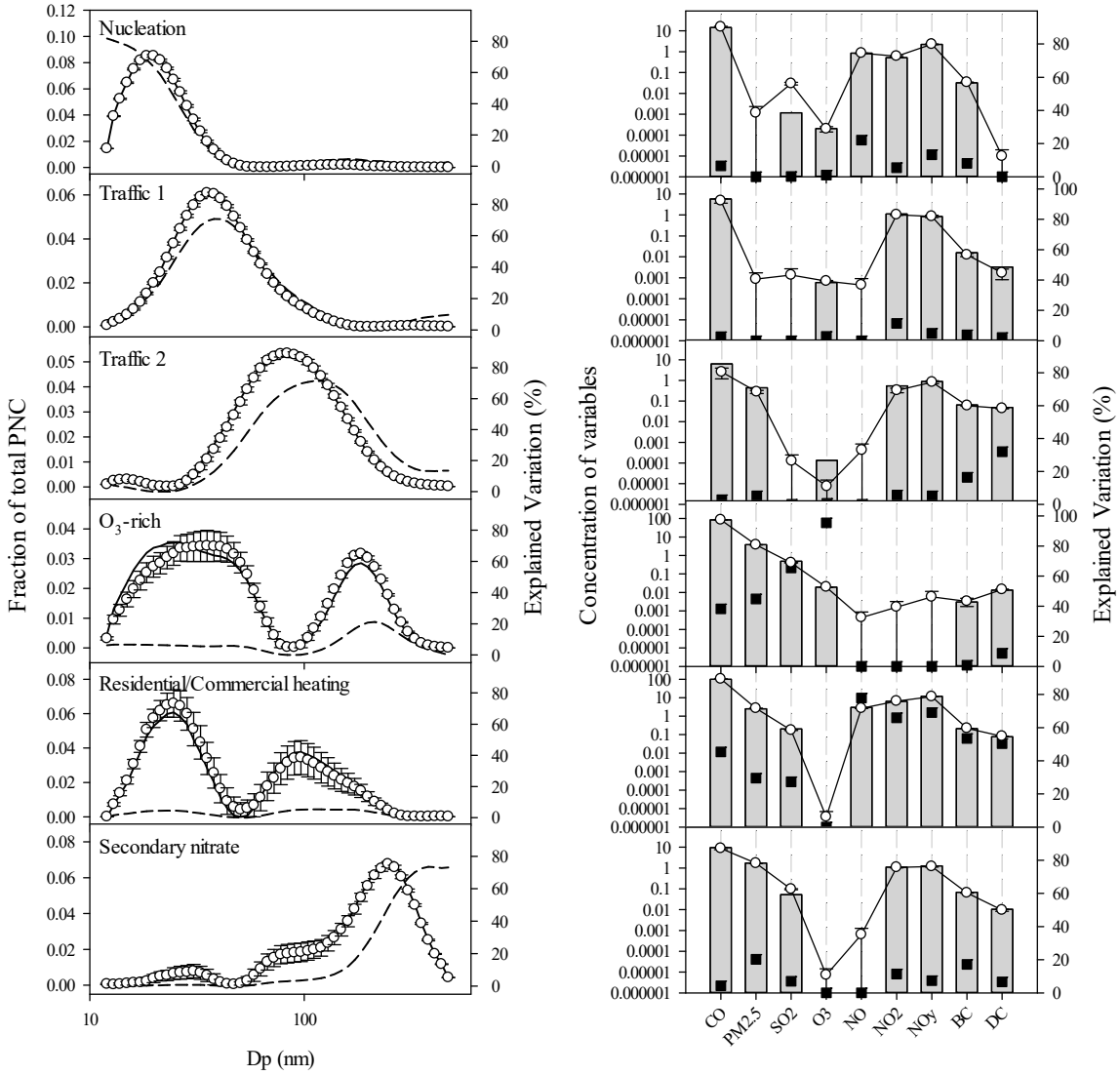

Figure 2. Profiles for the sources resolved from the data collected in December, January, and February 2011–2013 in Rochester, NY. Particle number size distributions (PNSD) profiles: The black solid lines present the normalized fractions on the total PNC, the open circles are the mean fractional displacement (DISP) values, the error bars represent the minimum and maximum fractional DISP values, and the dashed lines present the % explained variation Species profiles: The bars present the base case values, the open circles are the mean DISP values, the error bars represent the minimum and maximum DISP values, and the filled squares present the % explained variation.

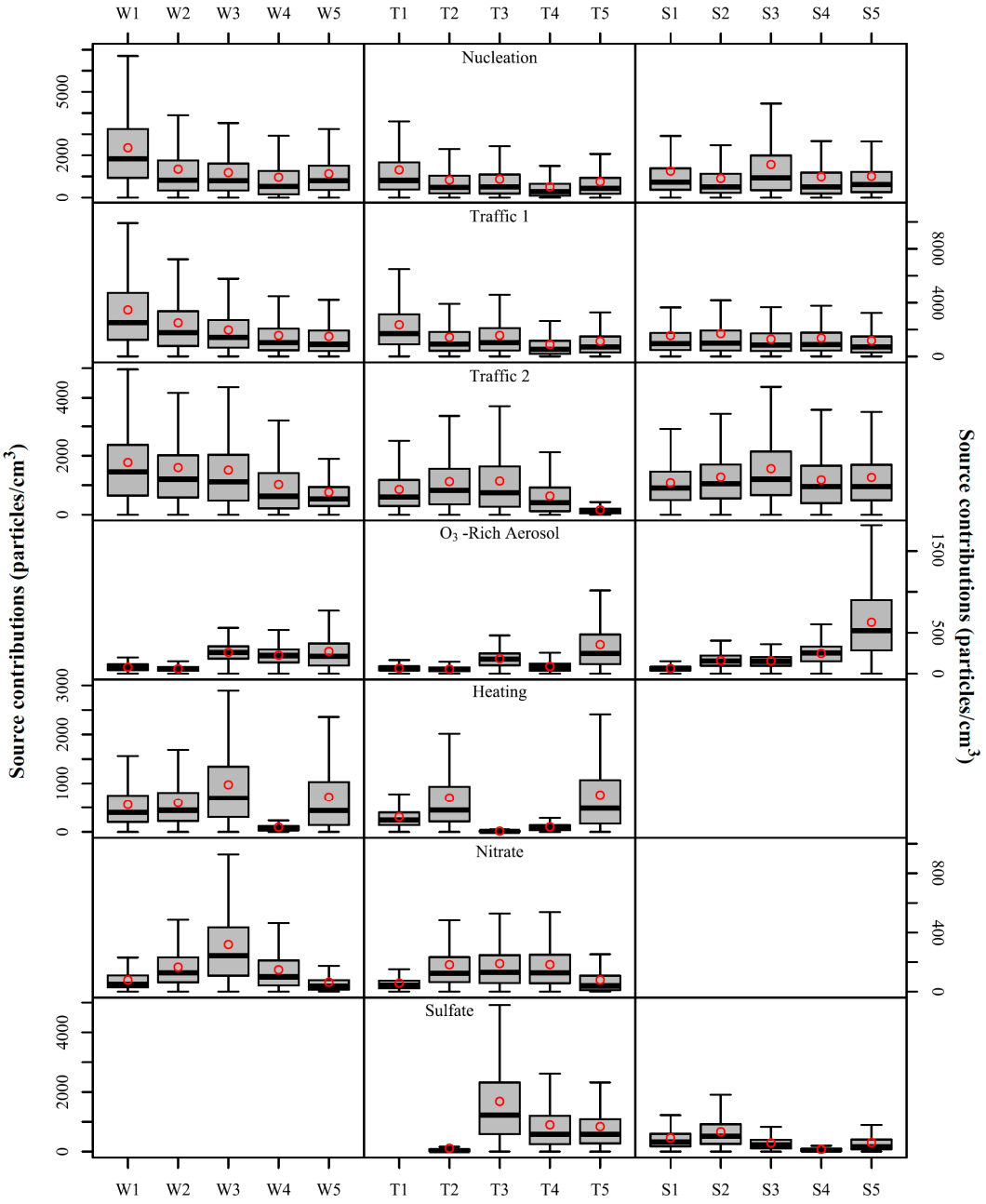

Figure 3. Average and ranges of concentrations of commonly identified sources as boxplots by season (W, T, and S) and by period (1–5) as defined in Table 1 (line = median, red circle = mean, box = interquartile range, whiskers = ±1.5*interquartile range).

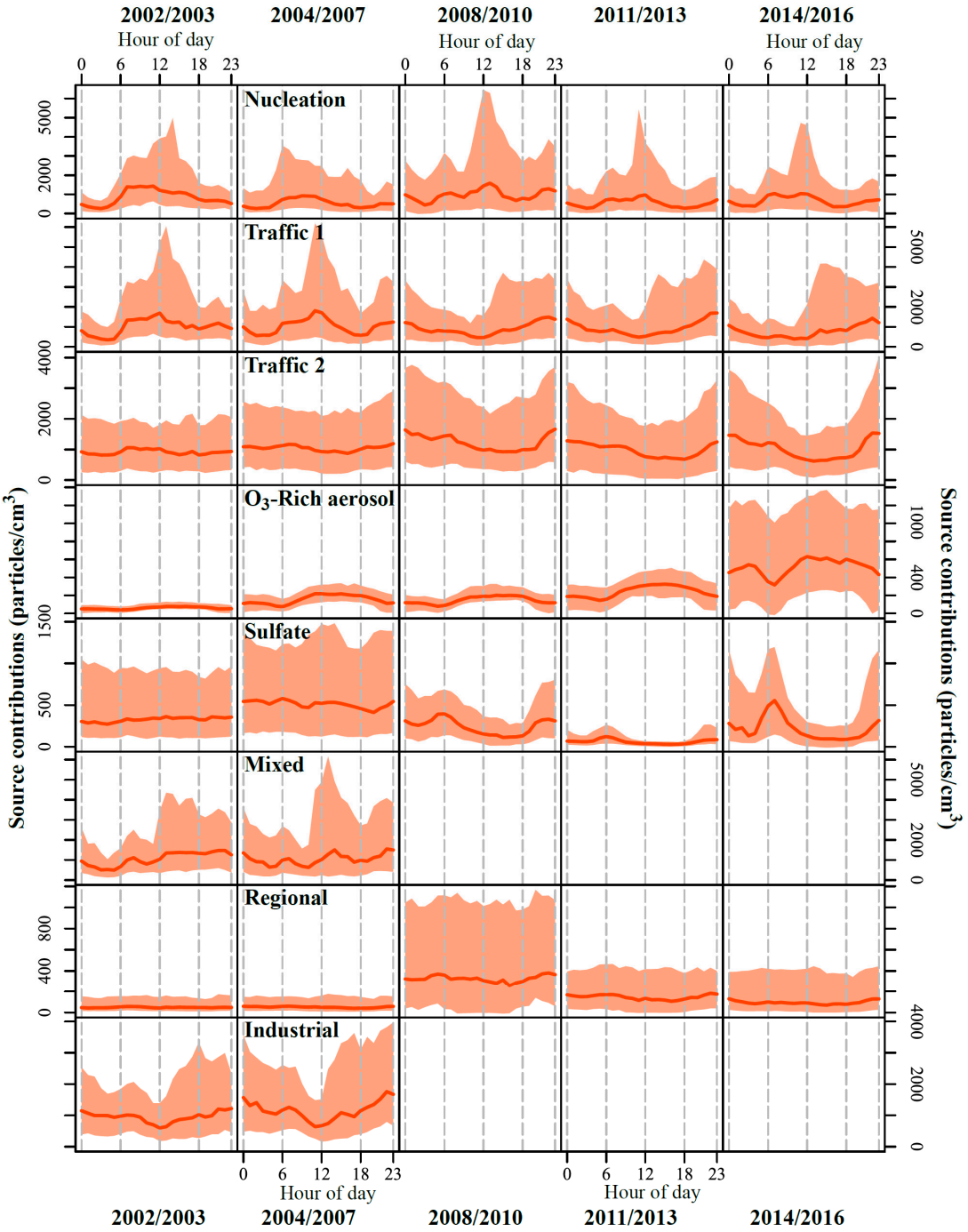

Figure 4. Diel variations of the identified sources during summer. Each plot reports the hourly average source contribution as a filled line and the associated 75th and 99th confidence intervals calculated by bootstrapping the data (n = 200).

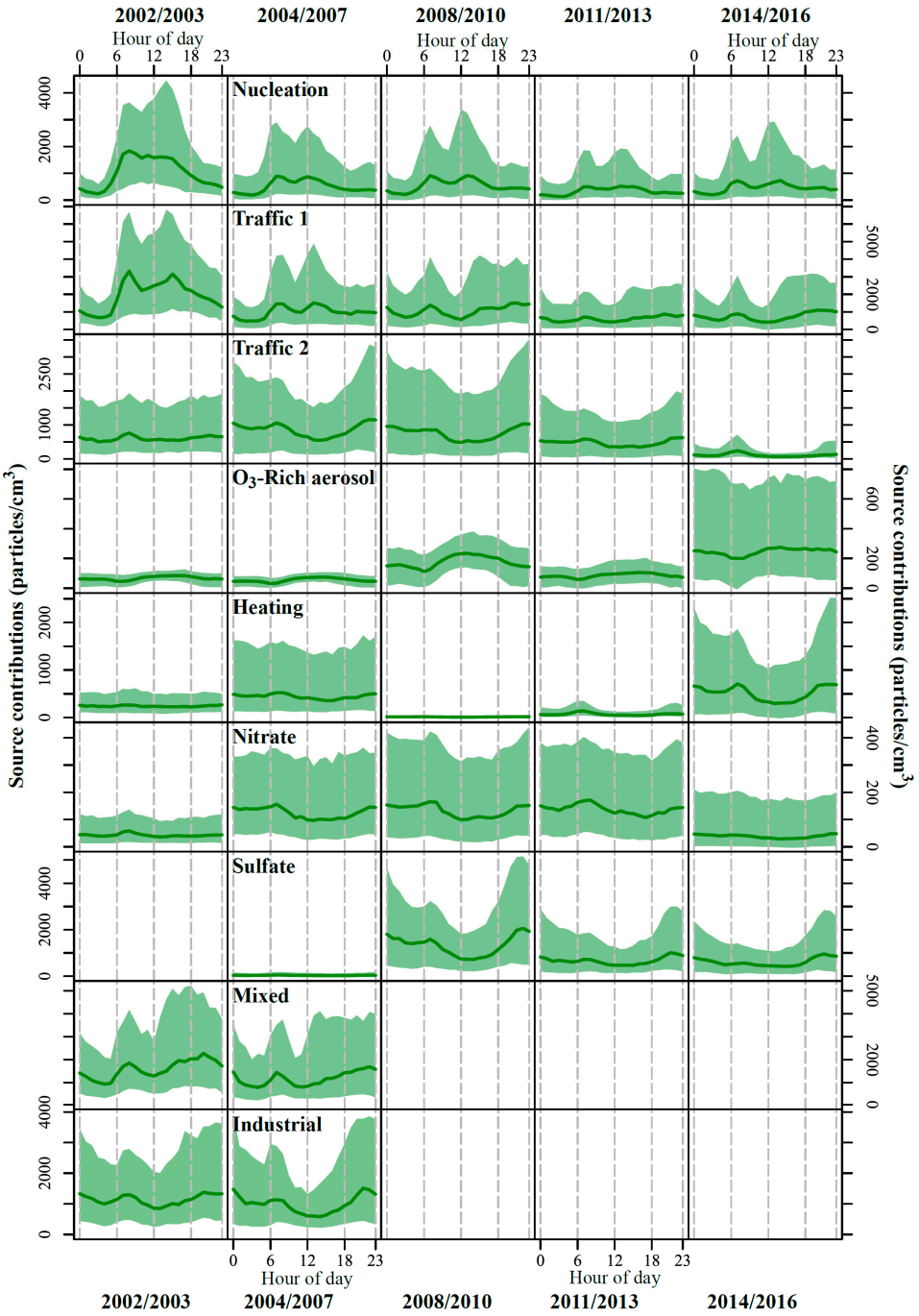

Figure 5. Diel variations of the identified sources during the transition period. Each plot reports the hourly average source contribution as a filled line and the associated 75th and 99th confidence intervals calculated by bootstrapping the data (n = 200).

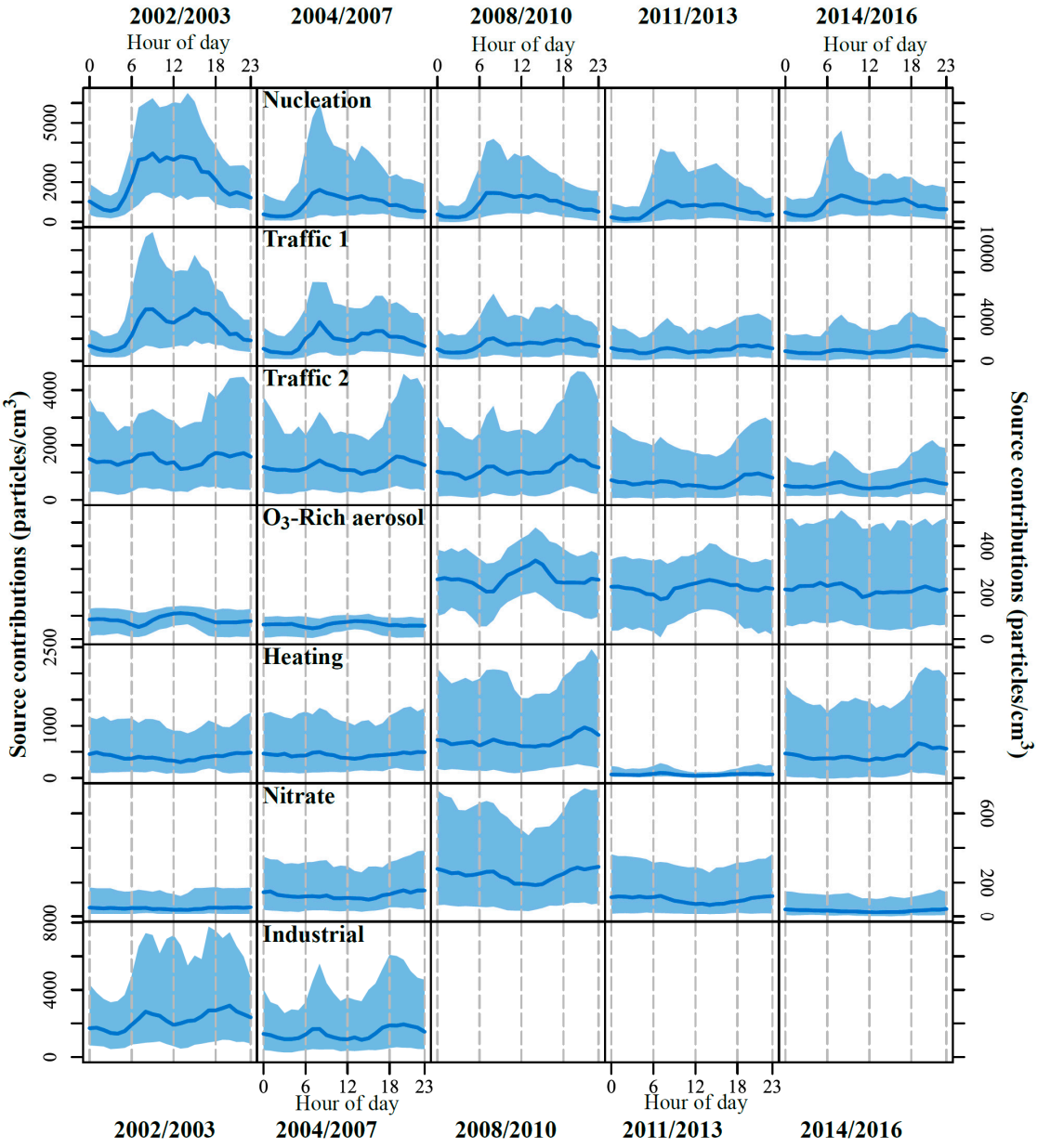

Figure 6. Diel variations of the identified sources during winter. Each plot reports the hourly average source contribution as a filled line and the associated 75th and 99th confidence intervals calculated by bootstrapping the data (n = 200).

3.1.1. Nucleation

This factor exhibited a single mode in the number distribution ranging from 14 to 25 nm, representing particles in the nucleation mode (Figures S1–S3). The highest contributions of PNC were observed during the daytime, with two peaks, one the morning and one around noon during summer, and in the morning and the afternoon during the winter and transition months. Similar profiles and daily patterns have been also reported in London [44–46]; Los Angeles [47,48], and Venice [49]. The noon/afternoon peak is driven by the enhanced photochemistry whereas the morning peak is likely vehicular emissions that nucleate as the emissions dilute and cool [29,44]. The presence of NO and SO_2 in these profiles supports the attribution of the nucleation mode particles largely to local vehicular traffic including the diesel rail line adjacent to the site. There were generally higher nucleation contributions on weekdays compared to weekends (Figures S21–S23), but there was not a consistently high weekday. The average nucleation contribution to PNC ranged from 11% (transition 2004–2007) to

29% (summer 2008–2010). There are similar concentrations of nucleation particles in the winter and summer again suggesting two mechanisms for their formation. In the winter, nucleation mode particles are highest during high traffic periods and under poor dispersion conditions (low wind speeds and mixing layer heights). In the summer, there is the midday-afternoon peak from photochemical activity leading to new particle formation. Both processes result in elevated concentrations of these smallest mode particles.

3.1.2. Traffic 1 and Traffic 2

Two traffic factors, traffic 1 (Figures S4–S6) and traffic 2 (Figures S7–S9), were identified showing major number modes around 30–35 nm and 58–104 nm, respectively, and slightly coarser particles during summer months. Along with nucleation, they represented the largest contributors to PNC (Table 1). Traffic 1 showed a clear peak in the morning (7–8) and high contributions more broadly distributed during the afternoon. On a day of week basis (Figures S21–S23), weekdays exhibited higher contributions compared to weekend days. Traffic 2 also showed a morning rush hour peak, but it had higher contributions during the night. The overnight peak may represent emissions from the adjacent railroad and a switching yard about 1.5 km northwest of the sampling site. Zhang et al. [50] reported that the dominant wind direction for high nighttime BC almost perfectly aligned with the railway line and that nighttime idling and switching activities of diesel locomotives in the railway yard led to the observed elevated BC concentrations.

Two distinct traffic factors with similar profiles and temporal patterns were reported by Zhou et al. [34,51] in Pittsburgh and by Sowlat et al. [47] in Los Angeles. Brines et al. [52] identified different traffic profiles in Barcelona, Madrid (Spain), and Brisbane (Australia). Similarly, two traffic factors were identified by Masiol et al. [46] at a site close to Heathrow Airport (London, UK). Traffic 1 generally represented the fresh-emitted traffic particles (in the finest mode) and includes CO, whereas traffic 2 was attributed to more aged particles [34]. However, Traffic 2 exhibited higher concentrations of BC, DC, CO, $PM_{2.5}$, and NO_y suggesting that traffic 2 is attributable in part to diesel emissions including the locomotives on the rail line adjacent to the monitoring site.

3.1.3. O_3-rich Secondary Aerosol

This factor had the highest explained variations for O_3 and high concentrations of O_3, $PM_{2.5}$, and CO with an average contribution to PNC of 5 $\pm$ 3% during the 2002–2016 period (Figures S10–S12). However, the size distributions presented multiple modes across the whole size range with different patterns in different periods and seasons. The diel patterns showed the highest contributions during the daytime following the solar radiation pattern that drives ozone formation. On a day of week basis, the highest contributions were observed during the weekend and during summer months. This pattern is consistent with the ozone patterns reported by Emami et al. [24] for Rochester and by Squizzato et al. [25] for sites across NYS. This factor is difficult to fully interpret. It shows varying patterns in its modal structure. The accumulation mode was strongest in the summer and transition seasons given the large DISP intervals observed for the ultrafine modes such as in the 01–10 transition period profile. This size particle is typically associated with transported secondary aerosol. In winter, the primary mode clearly shifts below 100 nm (ultrafine). Given the lower rate of formation of sulfate and secondary organic aerosol (SOA) in the winter with lower temperatures and less photochemical activity, these particles could still represent a transported secondary aerosol. These larger secondary particles would support the observed high contributions to the $PM_{2.5}$ mass concentrations. In a recent study of these particle size distributions measured between January 2012 and December 2014 with the addition of speciated mercury concentrations [53], they used potential source contribution function analysis and found that the O_3-rich factor appeared to be associated with non-ferrous metal smelters in Canada and the Toronto metropolitan area. Further research that would include highly time resolved compositional data will be required to understand what this factor represents.

3.1.4. Residential/Commercial Heating

The residential/commercial heating profiles (Figures S13 and S14) had two major modes; the smaller sized mode between 20 and 33 nm and a coarser mode between 111 and 138 nm. This factor was extracted only during the winter and transition periods. It was characterized by a high explained variation of BC, DC, and SO_2. Species profiles also exhibited contributions of PM, BC, DC, and NO_y. Median contributions did not show strong day of the week patterns. It showed highest contributions during nighttime. Associated species and diel pattern support the assignment to emissions from heating including emissions from natural gas and wood combustion, explaining the high NO_y and DC concentrations, respectively.

Natural gas is the primary fuel in the city for domestic and commercial space heating [54]. Wood combustion for space heating increased during the period. It was estimated that housing units burning wood for space heating fuel increased from 1475 in 2000 [54] to 2035 in 2009 [54]. However, most of the wood burning is recreational with the highest contributions of wood smoke to $PM_{2.5}$ occurring on weekends [31]. No. 2 oil is the other major heating fuel and is used in areas without a ready access to natural gas. All distillate oil sold in NYS for any purpose after 1 July 2012 had to be ultralow sulfur. The contributions of home heating oil and coal combustion in the Kodak Park cogeneration facility are consistent with the explained variation of SO_2 in the profiles.

3.1.5. Secondary Nitrate

Secondary nitrate profiles had three modes in the particles number profiles with the major number mode between 210 and 305 nm and high explained variation for particles in the accumulation mode (Figures S15 and S16). The other modes were in the ultrafine and Aitken mode size ranges. The species profiles showed high concentrations of $PM_{2.5}$, BC, and DC. The presence of both ultrafine and accumulation mode particles suggests that both local and distant particle sources may be contributing to this factor [30]. The presence of the nucleation mode is similar to the observations in Pittsburgh by Zhou et al. [51] where hourly nitrate values were available and present in the analogous factor profile that included the nitrate in the analysis. This source was identified only during winter and transition months with the highest contributions during nighttime and early morning when conditions are best for particulate nitrate formation and low contributions to PNC ($3 \pm 2\%$ on average), again similar to what was observed in Pittsburgh [51]. As previously observed by Dall'Osto et al. [55,56] and Masiol et al. [49], increased contributions during the night are consistent with the heterogeneous reactions of N_2O_5 and NO_3 on the particle surfaces [11]. The particles in the nucleation and Aitken mode were likely associated with the gas-to-particle conversion of local NO_x emissions [51] whereas the accumulation mode particles could be formed during the transport and reactions of its precursor gases, NH_3 and NO_x [30]. Zhao et al. [57] in their study of the midwestern US found that in metropolitan areas, there was higher nitrate than in rural areas suggesting the importance of local NO_x emissions and conversion to gaseous HNO_3. The presence of BC and DC in the species profile is likely related to the condensation of secondary nitrate particles on pre-existing BC and DC particles.

3.1.6. Secondary Sulfate

A factor representing secondary sulfate was resolved only for the summer and transitional periods (Figures S17 and S18). It represents ~ 6% and ~ 25% of the PNC during summer and transition periods, respectively. It had its highest concentrations at night. It was characterized by a major mode at ~72 nm during transition, whereas summer periods exhibited varying source profiles. However, species profiles show high concentrations of $PM_{2.5}$, SO_2, BC, and DC. The association of this factor with particles smaller than 200 nm suggests the sulfate formation is primarily through homogeneous (gas phase) processes [38,58]. The summer profiles exhibited larger particles compared to the transition ones (Figures S17 and S18) suggesting a greater contribution from cloud processed sulfate as well as the greater level of homogeneous photochemical activity.

There was a discernable shift downward in the size of the main mode over time. Squizzato et al. [25] reported a very sharp drop in the concentrations of SO_2 and sulfate over the 2005 to 2016 period and it might be anticipated that as the mass of sulfate decreased, the average particle size also became smaller. In the 2008–10 and 2014–16 summer profiles, an additional smaller size mode was found. In the earlier period, there could be sufficient local SO_2 emissions from coal and non-road diesel fuel combustion to result in small particle formation. However, the reasons for the presence of the smaller mode in the most recent period are uncertain. It could represent secondary organic aerosol (SOA) since other work has found that has increased at the end of the study period and the SOA was strongly correlated with spark-ignition vehicle emissions [59]. Given the monitoring sites proximity to major highways, SOA contributions to this factor profile is possible.

3.1.7. Regionally Transported Aerosol

A regional transport factor was only resolved for the summer periods and it was mainly characterized by accumulation mode particles (Figure S19). However, the resolved profiles also showed minor modes with particles in the Aitken and nucleation size range. This factor explained ~ 4% of PNC and was associated with high concentrations of $PM_{2.5}$ and BC. No significant diel variations or day-of-week patterns were observed suggesting no significant local contributions. Particles in the accumulation mode can be transported over long distances because they are too small to deposit by inertial and gravitational processes and too large to diffuse ([60] and references therein). Wang et al. [26] observed a high number of particles in the 100–500 nm range associated with regional polluted air parcels transported from the Ohio River Valley, a high SO_2 emission area in the Eastern US [61]. Thus, this factor likely represented sulfate particles formed during the long-range transport of air masses enriched in SO_2.

4. Conclusions

In the last two decades, the northeastern United States has experienced significant emissions reductions because of adopted mitigation strategies and economic drivers that led to decreases in $PM_{2.5}$, major gaseous pollutants concentrations (SO_2, CO, NO_x), and ultrafine particles (UFPs) [24,25,28]. During this period, the US also experienced one of the worst financial/economic crises of the last century and a shift in electricity generation away from coal combustion. Within the 2002 to 2016 period, eight sources of particles measured in Rochester were identified: Nucleation, two traffic factors (traffic 1 and traffic 2), residential/commercial heating, O_3-rich secondary aerosol, secondary nitrate, secondary sulfate, and regionally transported aerosol. There has been a general reduction in the particle number concentrations [28], and some changes in the source profiles of some of the sources as fuel compositions have changed and additional controls have been implemented on heavy-duty diesel-powered vehicles.

Supplementary Materials: The following are available online at http://www.mdpi.com/2073-4433/10/1/27/s1, Figures S1–S23 as called out in the text showing the additional source profiles, contribution distributions, and temporal variations.

Author Contributions: M.M., S.S., and F.E. were involved in the data analysis and interpretation of the results; D.C.C. assisted in the data collection, review, and validation; M.J.U. and D.Q.R. assisted in the interpretation of the results; P.K.H. supervised the project and assisted in the interpretation of the results. All of the authors were involved in the preparation and review of the manuscript.

Funding: This work was supported by the New York State Energy Research and Development Authority (NYSERDA) under agreement #59802 and the National Institute of Environmental Health Sciences (grant no. P30ES001247).

Acknowledgments: The authors gratefully acknowledge U.S. EPA and NYS DEC for the air pollutant data and for hosting our SMPS operational at the DEC site.

Conflicts of Interest: The authors declare no conflicts of interest.

References

1. Solomon, P.A.; Crumpler, D.; Flanagan, J.B.; Jayanty, R.K.M.; Rickman, E.E.; McDade, C.E. US national PM2.5 chemical speciation monitoring networks—CSN and IMPROVE: Description of networks. *J. Air Waste Manag. Assoc.* **2014**, *64*, 1410–1438. [CrossRef] [PubMed]
2. Oberdörster, G.; Oberdörster, E.; Oberdörster, J. Nanotoxicology: An emerging discipline evolving from studies of ultrafine particles. *Environ. Health Perspect.* **2005**, *113*, 823–839. [CrossRef] [PubMed]
3. Knibbs, L.D.; Cole-Hunter, T.; Morawska, L. A review of commuter exposure to ultrafine particles and its health effects. *Atmos. Environ.* **2011**, *45*, 2611–2622. [CrossRef]
4. Strak, M.; Janssen, N.A.; Godri, K.J.; Gosens, I.; Mudway, I.S.; Cassee, F.R.; Lebret, E.; Kelly, F.J.; Harrison, R.M.; Brunekreef, B.; et al. Respiratory health effects of airborne particulate matter: The role of particle size, composition, and oxidative potential-the RAPTES project. *Environ. Health Perspect.* **2012**, *120*, 1183–1189. [CrossRef] [PubMed]
5. Rich, D.Q.; Zareba, W.; Beckett, W.; Hopke, P.K.; Oakes, D.; Frampton, M.W.; Bisognano, J.; Chalupa, D.; Bausch, J.; O'Shea, K.; et al. Are ambient ultrafine, accumulation mode, and fine particles associated with adverse cardiac responses in patients undergoing cardiac rehabilitation? *Environ. Health Perspect.* **2012**, *120*, 1162–1169. [CrossRef]
6. Ostro, B.; Hu, J.; Goldberg, D.; Reynolds, P.; Hertz, A.; Bernstein, L.; Kleeman, M.J. Associations of mortality with long-term exposures to fine and ultrafine particles, species and sources: Results from the California teachers study cohort. *Environ. Health Perspect.* **2015**, *123*, 549–556. [CrossRef]
7. Lanzinger, S.; Schneider, A.; Breitner, S.; Stafoggia, M.; Erzen, I.; Dostal, M.; Pastorkova, A.; Bastian, S.; Cyrys, J.; Zscheppang, A.; et al. Associations between ultrafine and fine particles and mortality in five central European cities—Results from the UFIREG study. *Environ. Int.* **2016**, *88*, 44–52. [CrossRef]
8. Zhang, R.; Khalizov, A.; Wang, L.; Hu, M.; Xu, W. Nucleation and growth of nanoparticles in the atmosphere. *Chem. Rev.* **2012**, *112*, 1957–2011. [CrossRef] [PubMed]
9. Kulmala, M.; Petäjä, T.; Ehn, M.; Thornton, J.; Sipilä, M.; Worsnop, D.R.; Kerminen, V.-M. Chemistry of atmospheric nucleation: On the recent advances on precursor characterization and atmospheric cluster composition in connection with atmospheric new particle formation. *Annu. Rev. Phys. Chem.* **2014**, *65*, 21–37. [CrossRef]
10. George, C.; Ammann, M.; D'Anna, B.; Donaldson, D.J.; Nizkorodov, S.A. Heterogeneous photochemistry in the atmosphere. *Chem. Rev.* **2015**, *115*, 4218–4258. [CrossRef]
11. Seinfeld, J.H.; Pandis, S.N. *Atmospheric Chemistry and Physics: From Air Pollution to Climate Change*, 3rd ed.; John Wiley & Sons: Hoboken, NJ, USA, 2016.
12. Jeong, C.H.; Hopke, P.K.; Chalupa, D.; Utell, M. Characteristics of nucleation and growth events of ultrafine particles measured in Rochester, NY. *Environ. Sci. Technol.* **2004**, *38*, 1933–1940. [CrossRef] [PubMed]
13. Kumar, P.; Morawska, L.; Birmili, W.; Paasonen, P.; Hu, M.; Kulmala, M.; Harrison, R.M.; Norford, L.; Britter, R. Ultrafine particles in cities. *Environ. Int.* **2014**, *66*, 1–10. [CrossRef] [PubMed]
14. Karjalainen, P.; Pirjola, L.; Heikkila, J.; Lahde, T.; Tzamkiozis, T.; Ntziachristos, L.; Keskinen, L.; Ronkko, T. Exhaust particles of modern gasoline vehicles: A laboratory and an on-road study. *Atmos. Environ.* **2014**, *97*, 262–270. [CrossRef]
15. Masiol, M.; Harrison, R.M. Aircraft engine exhaust emissions and other airport-related contributions to ambient air pollution: A review. *Atmos. Environ.* **2014**, *95*, 409–455. [CrossRef]
16. Anderson, M.; Salo, K.; Hallquist, Å.M.; Fridell, E. Characterization of particles from a marine engine operating at low loads. *Atmos. Environ.* **2015**, *101*, 65–71. [CrossRef]
17. Jeong, C.H.; Traub, A.; Evans, G.J. Exposure to ultrafine particles and black carbon in diesel-powered commuter trains. *Atmos. Environ.* **2017**, *155*, 46–52. [CrossRef]
18. Riffault, V.; Arndt, J.; Marris, H.; Mbengue, S.; Setyan, A.; Alleman, L.Y.; Deboudt, K.; Flament, P.; Augustin, P.; Delbarre, H. Fine and ultrafine particles in the vicinity of industrial activities: A review. *Crit. Rev. Environ. Sci. Technol.* **2015**, *45*, 2305–2356. [CrossRef]
19. Kheirbek, I.; Haney, J.; Douglas, S.; Ito, K.; Caputo, S., Jr.; Matte, T. The public health benefits of reducing fine particulate matter through conversion to cleaner heating fuels in New York City. *Environ. Sci. Technol.* **2014**, *48*, 13573–13582. [CrossRef]

20. Buonanno, G.; Morawska, L. Ultrafine particle emission of waste incinerators and comparison to the exposure of urban citizens. *Waste Manag.* **2015**, *37*, 75–81. [CrossRef]
21. Chandrasekaran, S.R.; Hopke, P.K.; Newtown, M.; Hurlbut, A. Residential-scale biomass boiler emissions and efficiency characterization for several fuels. *Energy Fuel* **2013**, *27*, 4840–4849. [CrossRef]
22. Kumar, P.; Pirjola, L.; Ketzel, M.; Harrison, R.M. Nanoparticle emissions from 11 nonvehicle exhaust sources—A review. *Atmos. Environ.* **2013**, *67*, 252–277. [CrossRef]
23. Duncan, B.N.; Lamsal, L.N.; Thompson, A.M.; Yoshida, Y.; Lu, Z.; Streets, D.G.; Hurwitz, M.M.; Pickering, K.E. A space-based, high-resolution view of notable changes in urban NOx pollution around the world (2005–2014). *J. Geophys. Res.-Atmos.* **2016**, *121*, 976–996. [CrossRef]
24. Emami, F.; Masiol, M.; Hopke, P.K. Air pollution at Rochester, NY: Long-term trends and multivariate analysis of upwind SO2 source impacts. *Sci. Total Environ.* **2018**, *612*, 1506–1515. [CrossRef] [PubMed]
25. Squizzato, S.; Masiol, M.; Rich, D.Q.; Hopke, P.K. $PM_{2.5}$ and gaseous pollutants in New York State during 2005–2016: Spatial variability, temporal trends, and economic influences. *Atmos. Environ.* **2018**, *183*, 209–224. [CrossRef]
26. Wang, Y.; Hopke, P.K.; Chalupa, D.C.; Utell, M.J. Long-term study of urban ultrafine particles and other pollutants. *Atmos. Environ.* **2011**, *45*, 7672–7680. [CrossRef]
27. Wang, Y.; Hopke, P.K.; Chalupa, D.C.; Utell, M.J. Effect of the Shutdown of a Coal-Fired Power Plant on Urban Ultrafine Particles and Other Pollutants. *Aerosol Sci. Technol.* **2011**, *45*, 1245–1249. [CrossRef]
28. Masiol, M.; Squizzato, S.; Chalupa, D.C.; Utell, M.J.; Rich, D.Q.; Hopke, P.K. Long-term trends in submicron particle concentrations in a metropolitan area of the northeastern United States. *Sci. Total Environ.* **2018**, *633*, 59–70. [CrossRef]
29. Ogulei, D.; Hopke, P.K.; Chalupa, D.C.; Utell, M.J. Modeling Source Contributions to Submicron Particle Number Concentrations Measured in Rochester, New York. *Aerosol Sci. Technol.* **2007**, *41*, 179–201. [CrossRef]
30. Kasumba, J.; Hopke, P.K.; Chalupa, D.C.; Utell, M.J. Comparison of sources of submicron particle number concentrations measured at two sites in Rochester, NY. *Sci. Total Environ.* **2009**, *407*, 5071–5084. [CrossRef]
31. Wang, Y.; Hopke, P.K.; Xia, X.; Rattigan, O.V.; Chalupa, D.C.; Utell, M.J. Source apportionment of airborne particulate matter using inorganic and organic species as tracers. *Atmos. Environ.* **2012**, *55*, 525–532. [CrossRef]
32. Emami, F.; Hopke, P.K. Effect of Adding Variables on Rotational Ambiguity in Positive Matrix Factorization Solutions. *Chemom. Intell. Lab. Syst.* **2017**, *62*, 198–202. [CrossRef]
33. Zhou, L.; Kim, E.; Hopke, P.K.; Stanier, C.; Pandis, S.N. Advanced factor analysis on Pittsburgh particle size distribution data. *Aerosol Sci. Technol.* **2004**, *38* (Suppl. 1), 118–132. [CrossRef]
34. Zhou, L.; Hopke, P.K.; Stanier, C.; Pandis, S.N. Mining airborne particulate size distribution data by positive matrix factorization. *J. Geophys. Res.* **2005**, *110*, D07S19. [CrossRef]
35. Paatero, P.; Tapper, U. Positive matrix factorization: A non-negative factor model with optimal utilization of error estimates of data values. *Environmetrics* **1994**, *5*, 111–126. [CrossRef]
36. Paatero, P. Least squares formulation of robust non-negative factor analysis. *Chemom. Intell. Lab.* **1997**, *37*, 23–35. [CrossRef]
37. Hopke, P.K. Review of receptor modeling methods for source apportionment. *J. Air Waste Manag. Assoc.* **2016**, *66*, 237–259. [CrossRef] [PubMed]
38. Ogulei, D.; Hopke, P.K.; Zhou, L.; Pancras, P.; Nair, N.; Ondov, J.M. Source apportionment of Baltimore aerosol from combined size distribution and chemical composition data. *Atmos. Environ.* **2006**, *40*, S396–S410. [CrossRef]
39. Polissar, A.V.; Hopke, P.K.; Paatero, P.; Malm, W.C.; Sisler, J.F. Atmospheric aerosol over Alaska 2. Elemental composition and sources. *J. Geophys. Res.* **1998**, *103*, 19045–19057. [CrossRef]
40. Reff, A.; Eberly, S.I.; Bhave, P.V. Receptor modeling of ambient particulate matter data using positive matrix factorization: Review of existing methods. *J. Air Waste Manag. Assoc.* **2007**, *57*, 146–154. [CrossRef]
41. Belis, C.A.; Larsen, B.R.; Amato, F.; El Haddad, I.; Favez, O.; Harrison, R.M.; Hopke, P.K.; Nava, S.; Paatero, P.; Prévôt, A.; et al. *European Guide on Air Pollution Source Apportionment with Receptor Models*; JRC Reference Reports EUR26080 EN; Publications Office of the European Union: Luxembourg, 2014.
42. Brown, S.G.; Eberly, S.; Paatero, P.; Norris, G.A. Methods for estimating uncertainty in PMF solutions: Examples with ambient air and water quality data and guidance on reporting PMF results. *Sci. Total Environ.* **2015**, *518*, 626–635. [CrossRef]

43. Paatero, P.; Eberly, S.; Brown, S.G.; Norris, G.A. Methods for estimating uncertainty in factor analytic solutions. *Atmos. Meas. Tech.* **2014**, *7*, 781–797. [CrossRef]
44. Harrison, R.M.; Beddows, D.C.S.; Dall'Osto, M. PMF Analysis of Wide-Range Particle Size Spectra Collected on a Major Highway. *Environ. Sci. Technol.* **2011**, *45*, 5522–5528. [CrossRef] [PubMed]
45. Beddows, D.C.S.; Harrison, R.M.; Green, D.C.; Fuller, G.W. Receptor modelling of both particle composition and size distribution from a background site in London, UK. *Atmos. Chem. Phys.* **2015**, *15*, 10107–10125. [CrossRef]
46. Masiol, M.; Harrison, R.M.; Vu, T.V.; Beddows, D.C.S. Sources of sub-micrometre particles near a major international airport. *Atmos. Chem. Phys.* **2017**, *17*, 12379–12403. [CrossRef]
47. Sowlat, M.H.; Hasheminassab, S.; Sioutas, C. Source apportionment of ambient particle number concentrations in central Los Angeles using positive matrix factorization (PMF). *Atmos. Chem. Phys.* **2016**, *16*, 4849–4866. [CrossRef]
48. Mousavi, A.; Sowlat, M.H.; Sioutas, C. Diurnal and seasonal trends and source apportionment of redox-active metals in Los Angeles using a novel online metal monitor and Positive Matrix Factorization (PMF). *Atmos. Environ.* **2018**, *174*, 15–24. [CrossRef]
49. Masiol, M.; Vu, T.V.; Beddows, D.C.S.; Harrison, R.M. Source apportionment of wide range particle size spectra and black carbon collected at the airport of Venice (Italy). *Atmos. Environ.* **2016**, *139*, 56–74. [CrossRef]
50. Zhang, K.M.; Allen, G.; Hopke, P.K.; Schwab, J.; Rattigan, O.V.; Felton, H.D. Long-Term, Continuous Aethelometer Monitoring Data Reveal Unexpected Black Carbon and Brown Carbon Sources. In Proceedings of the 10th International Aerosol Conference, St. Louis, MO, USA, 2–7 September 2018.
51. Zhou, L.; Hopke, P.K.; Stanier, C.; Pandis, S.N.; Ondov, J.M.; Pancras, J.P. Investigation of the relationship between chemical composition and size distribution of airborne particles by partial least squares (PLS) and positive matrix factorization (PMF). *J. Geophys. Res.* **2005**, *110*, D07S18. [CrossRef]
52. Brines, M.; Dall'Osto, M.; Beddows, D.C.S.; Harrison, R.M.; Gómez-Moreno, F.; Núñez, L.; Artíñano, B.; Costabile, F.; Gobbi, G.P.; Saliimi, F.; et al. Traffic and nucleation events as main sources of ultrafine particles in high-insolation developed world cities. *Atmos. Chem. Phys.* **2015**, *15*, 5929–5945. [CrossRef]
53. Zhou, H.; Hopke, P.K.; Zhou, C.; Holsen, T.M. Ambient mercury source identification at a New York State urban site: Rochester, NY. *Sci. Total Environ.* **2019**, *650*, 1327–1337. [CrossRef]
54. NYSERDA. *New York State Energy Research and Development Authority—Patterns and Trends*; New York State Energy Profiles: 2000–2014 Final Report; NYSERDA: Albany, NY, USA, 2016. Available online: https://www.nyserda.ny.gov/About/Publications/EA-Reports-and-Studies/Patterns-and-Trends (accessed on 15 March 2018).
55. NYSERDA. *New York State Energy Research and Development Authority—Patterns and Trends*; 1993–2007, New York State Energy Profiles Albany; NYSERDA: Albany, NY, USA, 2009.
56. Dall'Osto, M.; Harrison, R.M.; Coe, H.; Williams, P.I.; Allan, J.D. Real time chemical characterization of local and regional nitrate aerosols. *Atmos. Chem. Phys.* **2009**, *9*, 3709–3720. [CrossRef]
57. Zhao, W.; Hopke, P.K.; Zhou, L. Spatial distribution of source locations for particulate nitrate and sulfate in the upper-midwestern United States. *Atmos. Environ.* **2007**, *41*, 1831–1847. [CrossRef]
58. John, W.; Wall, S.M.; Ondo, J.L.; Winklmayr, W. Modes in the Size Distributions of Atmospheric Inorganic Aerosol. *Atmos. Environ.* **1990**, *24*, 2349–2359. [CrossRef]
59. Squizzato, S.; Masiol, M.; Rich, D.Q.; Hopke, P.K. Long-term trends (2005–2016) of source apportioned $PM_{2.5}$ across New York State. *Atmos. Environ.* **2019**. [CrossRef]
60. Vu, T.V.; Delgado-Saborit, J.M.; Harrison, R.M. Review: Particle number size distributions from seven major sources and implications for source apportionment studies. *Atmos. Environ.* **2015**, *122*, 114–132. [CrossRef]
61. Hopke, P.K.; Zhou, L.; Poirot, R.L. Reconciling Trajectory Ensemble Receptor Model Results with Emissions. *Environ. Sci. Technol.* **2005**, *39*, 7980–7983. [CrossRef] [PubMed]